



Scaling Group Analysis on MHD Free Convective Heat and Mass Transfer over a Stretching Surface with Suction / Injection, Heat Source/Sink Considering Viscous Dissipation and Chemical Reaction Effects

Hunegnaw Dessie and Naikoti Kishan

Department of Mathematics

Osmania University

Hyderabad 500007

Andhra Pradesh, India

hunegnawd@yahoo.com; kishan_n@rediffmail.com

Received: June 10, 2014; Accepted: October 20, 2014

Abstract

This paper concerns with scaling group analysis on MHD free convective heat and mass transfer over stretching surface considering effects of thermal-diffusion and diffusion-thermo with suction /injection, heat source/sink and chemical reaction by taking into account viscous dissipation. Scaling group transformations are used to convert the partial differential equations of governing equations into ordinary differential equation and are solved numerically by Keller Box Method. Numerical results obtained for different parameters are drawn graphically and their effects on velocity, temperature and concentration profiles are discussed and shown graphically. Skin-friction coefficient, Nusselt number and Sherwood number are presented in table. It is noted that the skin-friction coefficient and mass transfer gradient decrease with the increase of Prandtl number but the temperature gradient increases. The effect of Eckert number and heat source parameter increases the skin-friction coefficient and the mass transfer gradient but decreases the temperature gradient.

Keywords: MHD, Lie group transformations; Heat and Mass transfer; Dufour and Soret effects; Keller Box method

MSC2010 No.: 34B15, 35 Q35, 76M20, 76R10, 76W05

1. Introduction

Flow of an incompressible viscous fluid over a stretching surface is a classical problem in fluid dynamics and important in various process. It is used to create polymers of fixed cross-sectional profiles, cooling of metallic and glass plates. Aerodynamics shaping of plastic sheet by forcing through die and boundary layer along a liquid film in condensation processes are among the other areas of applications. The production of sheeting material, which includes both metal and polymer sheets arises in a number of industrial manufacturing processes. First of all, Sakiadis (1961) investigated the boundary layer behavior on stretching surfaces and presented numerical solution for the sheet having constant speed. Extension to this problem where velocity is proportional to the distance from the slit was given by Crane (1970). Flow and heat transfer in the boundary layer on stretching surface was studied by Tsou et al. (1967). Fox et al. (1969) presented different methods analytical or numerical for solving problems of stretching sheet with suction and injection. The three dimensional flow past a stretching sheet by extended optimal homotopy asymptotic method is studied by Ullah et al. (2014). Heat and mass transfer on stretched surface with suction and injection was introduced by Erickson et al. (1966). Gupta and Gupta (1966) studied the same problem for linearly stretching sheet. Manjulatha et al. (2014) investigated effects of radiation absorption and mass transfer on the free convective flow passed a vertical flat plate through a porous medium in an aligned magnetic field. Heat transfer past a moving continuous plate with variable temperature was studied by Soundalgekar and Murty (1980), and Grubka and Bobba (1985).

Ali (1966) presented similarity solutions for stretched surface with suction and injection. Radiation effects on MHD stagnation point flow of nanofluid towards a stretching surface with convective boundary condition are investigated by NoreenSher et al. (2013). Gupta (1966) studied laminar free convection flow of an electrically conducting fluid from a vertical plate with uniform surface heat flux and variable wall temperature in the presence of a magnetic field. Effects of chemical reaction and radiation absorption on MHD flow of dusty viscoelastic fluid are studied by Prakash et al. (2014). Gorela and Abboud (1998) studied the MHD effect on a vertical stretching surface with suction and blowing. Chiam (1995) has discussed the hydrodynamic flow over a surface stretching with a power law velocity. Makinde et al. (2013) studied buoyancy effects on MHD stagnation point flow and heat transfer of a nanofluid past a convectively heated stretching/ shrinking sheet.

An energy flux can be generated not only due to the temperature gradients but also by composition gradients. The energy flux produced by a composition gradient is referred to as the diffusion thermo (Dufour) effect, whereas mass flux caused by temperature gradients is known as the thermal diffusion (Soret) effect. In general, the diffusion thermo effect and thermal-diffusion effect are of a smaller order of magnitude than the effects described by Fourier's or Fick's law. This is why most of the studies of heat and mass transfer processes, however, considered constant plate temperature and concentration and have neglected the diffusion-thermo and thermal-diffusion terms from the energy and concentration equations respectively. But in some exceptional cases, for instance, in mixture between gases with very light molecular weight (H_2 , He) and of medium molecular weight (N_2 , air) the diffusion-thermo (Dufour) effect and in isotope separation, the thermal-diffusion (Soret)

effect was found to be of a considerable magnitude such that these effects cannot be ignored. In view of the importance of this diffusion – thermo effect, similarity equations of the momentum energy and concentration equations are derived by introducing a time dependent length scale. In the view of the importance of the above mentioned effects, Dursunkay and Worek (1992) studied diffusion-thermo and thermal-diffusion effects in transient and steady natural convection from a vertical surface, whereas Kafoussias and Williams (1995) studied the same effects on mixed free-forced convective and mass transfer boundary layer flow with temperature dependent viscosity. Anghel et al. (2000) investigated the Dufour and Soret effects on free convection boundary layer over a vertical surface embedded in a porous medium. Poselnico (2004) studied numerically the influence of a magnetic field on heat and mass transfer by natural convection from vertical surfaces in porous media considering Soret and Dufour effects. Alam et al. (2005) studied the effects of Dufour and Soret numbers on unsteady free convection and mass transfer flow past an impulsively started infinite vertical porous flat plate of a viscous incompressible and electrically conducting fluid in the presence of a uniform transverse magnetic field. Alam et al. (2006) studied the effects of Dufour and Soret numbers on steady free-forced convective and mass transfer flow past a semi-infinite vertical flat plate in the presence of a uniform transverse magnetic field. Seddeek (2006) studied the thermal-diffusion and diffusion thermo effects on mixed free forced convective flow and mass transfer over accelerating surface with a heat source in the presence of suction and blowing in the case of variable viscosity.

Viscous dissipation changes the temperature distributions by playing a role like energy source which leads to affect heat transfer rates. The merit of the effect of viscous dissipation depends on whether the sheet is being cooled or heated. Gebhart (1962) has shown the importance of viscous dissipative heat in free convection flow in the case of isothermal and constant heat flux at the plate. Analytical solution for two-phase flow between two rotating cylinders filled with power-law liquid and a micro layer of gas is studied by Mohammed et al. (2014). Gebhart and Mollendorf (1969) considered the effects of viscous dissipation for external natural convection flow over a surface. Hajmohammed and Nourazar (2014) investigated on the insertion of a thin gas layer in micro cylindrical Couette flows filled with power-law liquids. Soundalgekar and Gakar analyzed viscous dissipative heat on the two-dimensional unsteady free convective flow past an infinite vertical porous plate when the temperature oscillates in time and there is constant suction at the plate. Israel Cookey et al. (2003) investigated the influence of viscous dissipation and radiation on unsteady MHD free convection flow past an infinite heated vertical plate in a porous medium with time dependent suction.

Combined heat and mass transfer flow in the presence of chemically reactive species concentration has bearing on many transport processes present in nature and also in science and engineering applications. In processes such as drying, evaporation, energy transfer in a cooling tower and the flow in a desert cooler, heat and mass transfer occur simultaneously. Free convection processes of involving the combined mechanism are also encountered in many natural processes and industrial applications such as in the curing of plastics, the cleaning and chemical processing of materials, the manufacturing of pulp and insulated cables. Chamkha (2003) studied MHD flow over a uniformly stretched vertical permeable surface subject to a chemical reaction. Afify (2004) analyzed the MHD free convective flow and mass transfer over a stretching sheet with a homogeneous chemical reaction of order n where n was taken to be 0, 1,

2, or 3. The influence of a chemical reaction on heat and mass transfer from vertical surfaces in porous media subject to Soret and Dufour effects was studied by Postelnicu (2007). Kandasamy and Palanimani (2007) studied the effects of a chemical reaction on heat and mass transfer on a magnetohydrodynamic boundary layer flow over a wedge with ohmic heating and viscous dissipation in a porous medium. Pal and Mondal (2011) studied the effects of Soret, Dufour, chemical reaction and thermal radiation on MHD non-Darcy unsteady mixed convective heat and mass transfer.

In this paper, by applying Lie's scaling' group transformations to the study of effects of thermal - diffusion and diffusion- thermo on MHD free convective heat and mass transfer over a stretching surface considering suction or injection by taking in to account viscous dissipation, heat source /sink and chemical reaction is analyzed. The system remains invariant due to some relations among the parameters of the transformations. With this transformation, a third order and a second order ordinary differential equations corresponding to momentum and energy equations are derived. These equations are solved with the help of power full, easy to use method called the Keller box method. This method has already been successfully applied to several non-linear problems corresponding to parabolic partial differential equations. As discussed in Keller (1971), the exact Discrete Calculus associated with the Keller box scheme is shown to be fundamentally different from all other mimic (physics capturing) numerical methods. The box-scheme of Keller (1971) is basically a mixed finite volume method, which consists in taking the average of a conservation law and of the associated constitutive law at the level of the same mesh cell. The equations (28)-(30) together with boundary conditions (31) can be also solved by semi-analytical means introduced in recent years such as homotopy, DTM and ADM which is explained very well in the paper Khan et al. (2008) and Ullah et al. (2013 & 2014). The effects of the flow parameters on velocity, temperature and concentration profiles are investigated and analyzed with the help of graphical representation

2. Governing equations

Consider a laminar and stable, steady free convective heat and mass transfer flow of a viscous incompressible electrically conducting fluid past a stretching surface coinciding with plane $y = 0$. The non-uniform transverse magnetic field $B(x)$ is imposed along y -axis and chemical reaction is taking place in the flow. The origin is kept fixed with equal and opposite forces applied along the x -axis which results in stretching of the sheet and hence the flow is generated. The temperature and the concentration of the ambient fluid are T_∞ and C_∞ , and those at the stretching surface are $T_w(x)$ and $C_w(x)$, respectively. In order to get the effect of temperature difference between the surface and the ambient fluid, we consider heat source/sink in the flow region. The induced magnetic field is neglected as the magnetic Reynolds number of the flow is taken very small. It is also assumed that the all body forces except the transverse magnetic forces are negligible. It is also assumed that the pressure gradient and the electrical dissipation are neglected. The fluid properties are assumed to be constant except the density in the buoyancy terms of the linear momentum equation which is approximated according to the Boussinesq's approximation. Under the above assumptions, the boundary layer form of equations can be written a (Dursunkaya and Worek (1992))

$$\frac{\partial u}{\partial x} + \frac{\partial v}{\partial y} = 0, \quad (1)$$

$$u \frac{\partial u}{\partial x} + v \frac{\partial u}{\partial y} = v \frac{\partial^2 u}{\partial y^2} - \frac{\sigma B_0^2(x)}{\rho} u + g B_T (T - T_\infty) + g B_C (C - C_\infty), \quad (2)$$

$$u \frac{\partial T}{\partial x} + v \frac{\partial T}{\partial y} = \alpha \frac{\partial^2 T}{\partial y^2} + \frac{D_m k_T}{C_s c_p} \frac{\partial^2 C}{\partial y^2} + \frac{Q_0}{\rho c_p} (T - T_\infty) + \frac{\mu}{\rho c_p} \left(\frac{\partial u}{\partial y}\right)^2, \quad (3)$$

$$u \frac{\partial C}{\partial x} + v \frac{\partial C}{\partial y} = D_m \frac{\partial^2 C}{\partial y^2} + \frac{D_m k_T}{T_m} \frac{\partial^2 T}{\partial y^2} - k^* (C - C_\infty), \quad (4)$$

where u, v are the velocity components in the x and y -directions, respectively, ν is the kinematic viscosity, σ is the electrical conductivity, ρ is the density of the fluid, B_T is the coefficient of thermal expansion, B_C is the coefficient of thermal expansion with concentration, T_m is the mean fluid temperature, T and T_m are the temperature of the fluid inside the thermal boundary layer and the fluid temperature in the free stream, respectively, while C and C_∞ are the corresponding concentrations, D_m is the coefficient of mass diffusivity, Q_0 is dimensional heat generation/absorption coefficient, μ is dynamic viscosity, c_p is specific heat capacity at constant pressure, k^* is dimensional chemical reaction coefficient, $B(x) = B_0 x^s$ is the applied magnetic field, α is the thermal diffusivity, k_T is the thermal-diffusion ratio and C_s is the concentration susceptibility.

2.1 Boundary conditions

The boundary conditions for equations (1)-(4) are expressed as

$$\begin{aligned} u(x, 0) = U(x) = C_1 x^m, \quad v(x) = v_w(x) = C_2 x^m, \quad T = T_w(x) = T_\infty + C_3 x^r, \\ C = C_w(x) = C_\infty + C_4 x^r, \quad u(x, \infty) = 0, \quad T(x, \infty) = T_\infty, \quad C(x, \infty) = C_\infty, \end{aligned} \quad (5)$$

where C_1, C_2, C_3, C_4 are the constants, $U(x)$ is the stretching speed of the plate, $v_w(x)$ is the transverse velocity at the surface.

2.2 Method of solution

We now introduce the following relations for u, θ and φ as follows

$$u = \frac{\partial \psi}{\partial y}, \quad v = -\frac{\partial \psi}{\partial x}, \quad \theta = \frac{T - T_\infty}{T_w - T_\infty} \quad \text{and} \quad \varphi = \frac{C - C_\infty}{C_w - C_\infty}, \quad (6)$$

where ψ is the stream function.

Then using equation (6), equations (2) - (4) can be written as

$$\frac{\partial \psi}{\partial y} \frac{\partial^2 \psi}{\partial x \partial y} - \frac{\partial \psi}{\partial x} \frac{\partial^2 \psi}{\partial y^2} = \nu \frac{\partial^3 \psi}{\partial y^3} - \frac{\sigma B_0^2 x^{2s} \partial \psi}{\rho \partial y} + g B_T C_3 \theta x^r + g B_C C_4 \varphi x^r, \quad (7)$$

$$\frac{\partial \psi}{\partial y} \left(r \frac{\theta}{x} + \frac{\partial \theta}{\partial x} \right) - \frac{\partial \psi}{\partial x} \frac{\partial \theta}{\partial y} = \alpha \frac{\partial^2 \theta}{\partial y^2} + \frac{D_m k_T (C_w - C_\infty)}{C_s c_p (T_w - T_\infty)} \frac{\partial^2 \varphi}{\partial y^2} + \frac{Q_0}{\rho c_p} \theta + \frac{\mu}{\rho c_p (T_w - T_\infty)} \left(\frac{\partial^2 \psi}{\partial y^2}\right)^2, \quad (8)$$

$$\frac{\partial \psi}{\partial y} \left(r \frac{\varphi}{x} + \frac{\partial \varphi}{\partial x} \right) - \frac{\partial \psi}{\partial x} \frac{\partial \varphi}{\partial y} = D_m \frac{\partial^2 \varphi}{\partial y^2} + \frac{D_m k_T (T_w - T_\infty)}{T_m (C_w - C_\infty)} \frac{\partial^2 \theta}{\partial y^2} - k^* \varphi, \quad (9)$$

and the boundary conditions of equation (5) can be written as

$$\begin{aligned} \frac{\partial \psi}{\partial y}(x, 0) &= C_1 x^m, \quad \frac{\partial \psi}{\partial x}(x, 0) = -C_2 x^m, \quad \theta(x, 0) = 1, \quad \varphi(x, 0) = 1, \\ \frac{\partial \psi}{\partial y}(x, \infty) &= 0, \quad \theta(x, \infty) = 0, \quad \varphi(x, \infty) = 0. \end{aligned} \quad (10)$$

2.3 Scaling group of transformations

Firstly, we shall derive the similarity solutions using the Lie group method under which the non-linear differential equations (7)-(9) and the boundary conditions (10) are invariant. The simplified form of the Lie-group transformation, namely the scaling groups of transformations given by Layek et al. (2006) are given by

$$\begin{aligned} \Gamma: \quad x^* &= x e^{\varepsilon \alpha_1}, \quad y^* = y e^{\varepsilon \alpha_2}, \quad \psi^* = \psi e^{\varepsilon \alpha_3}, \\ u^* &= u e^{\varepsilon \alpha_4}, \quad v^* = v e^{\varepsilon \alpha_5}, \quad \theta^* = \theta e^{\varepsilon \alpha_6}, \quad \varphi^* = \varphi e^{\varepsilon \alpha_7}, \end{aligned} \quad (11)$$

where $\alpha_1, \alpha_2, \alpha_3, \alpha_4, \alpha_5, \alpha_6$ and α_7 are transformation parameters.

Equation (11) may be considered as a point-transformation which transforms coordinates

$(x, y, \psi, u, v, \theta)$ to the coordinates $(x^*, y^*, \psi^*, u^*, v^*, \theta^*)$.

Substituting equation (11) into (7)-(9), we obtain

$$\begin{aligned} e^{\varepsilon(\alpha_1 + 2\alpha_2 - 2\alpha_3)} &\left(\frac{\partial \psi^*}{\partial y^*} \frac{\partial^2 \psi^*}{\partial x^* \partial y^*} - \frac{\partial \psi^*}{\partial x^*} \frac{\partial^2 \psi^*}{\partial y^{*2}} \right) \\ &= v e^{\varepsilon(3\alpha_2 - \alpha_3)} \frac{\partial^3 \psi^*}{\partial y^{*3}} - \frac{\sigma B_0^2}{\rho} e^{\varepsilon(\alpha_2 - 2s\alpha_1 - \alpha_3)} x^{*2s} \frac{\partial \psi^*}{\partial y^*} \\ &\quad + g B_T C_3 e^{\varepsilon(-r\alpha_1 - \alpha_6)} \theta^* x^{*r} + g B_C C_4 e^{\varepsilon(-r\alpha_1 - \alpha_7)} \varphi^* x^{*r}, \end{aligned} \quad (12)$$

$$\begin{aligned} e^{\varepsilon(\alpha_1 + \alpha_2 - \alpha_3 - \alpha_6)} &\left(r \frac{\partial \psi^*}{\partial y^*} \frac{\theta^*}{x^*} + \frac{\partial \psi^*}{\partial y^*} \frac{\partial \theta^*}{\partial x^*} - \frac{\partial \psi^*}{\partial x^*} \frac{\partial \theta^*}{\partial y^*} \right) = \alpha e^{\varepsilon(2\alpha_2 - \alpha_6)} \frac{\partial^2 \theta^*}{\partial y^{*2}} \\ &+ \frac{D_m k_T (C_w - C_\infty)}{C_s C_p (T_w - T_\infty)} e^{\varepsilon(2\alpha_2 - \alpha_7)} \frac{\partial^2 \varphi^*}{\partial y^{*2}} \\ &+ \frac{Q_0}{\rho c_p} \theta^* e^{-\varepsilon \alpha_6} + \frac{\mu}{\rho c_p (T_w - T_\infty)} e^{\varepsilon(4\alpha_2 - 2\alpha_3)} \left(\frac{\partial^2 \psi^*}{\partial y^{*2}} \right)^2, \end{aligned} \quad (13)$$

$$\begin{aligned}
 & e^{\varepsilon(\alpha_1+\alpha_2-\alpha_3-\alpha_7)} \left(r \frac{\partial \psi^*}{\partial y^*} \frac{\varphi^*}{x^*} + \frac{\partial \psi^*}{\partial y^*} \frac{\partial \varphi^*}{\partial x^*} - \frac{\partial \psi^*}{\partial x^*} \frac{\partial \varphi^*}{\partial y^*} \right) \\
 & = D_m e^{\varepsilon(2\alpha_2-\alpha_7)} \frac{\partial^2 \varphi^*}{\partial y^{*2}} - k^* \varphi^* e^{-\varepsilon\alpha_7} + \frac{D_m k_T (T_w - T_\infty)}{T_m (C_w - C_\infty)} e^{\varepsilon(2\alpha_2-\alpha_7)} \frac{\partial^2 \theta^*}{\partial y^{*2}} .
 \end{aligned} \tag{14}$$

The boundary conditions are

$$\begin{aligned}
 y = 0: & \quad e^{\varepsilon(\alpha_2-\alpha_3)} \frac{\partial \psi^*}{\partial y^*} = C_1 e^{-m\varepsilon\alpha_1} x^{*m}, \quad e^{\varepsilon(\alpha_1-\alpha_3)} \frac{\partial \psi^*}{\partial x^*} = -C_2 x^{*n} e^{-\varepsilon n\alpha_1}, \\
 & \quad \theta^* e^{-\varepsilon\alpha_6} = 1, \quad \varphi^* e^{-\varepsilon\alpha_7} = 1, \\
 y \rightarrow \infty: & \quad e^{\varepsilon(\alpha_2-\alpha_3)} \frac{\partial \psi^*}{\partial y^*} = 0, \quad \theta^* e^{-\varepsilon\alpha_6} = 0, \quad \varphi^* e^{-\varepsilon\alpha_7} = 0.
 \end{aligned} \tag{15}$$

However, the system of equations (12)-(15) remains invariant under the group of transformation Γ , if the following relations hold:

$$\begin{aligned}
 \alpha_1 + 2\alpha_2 - 2\alpha_3 = 3\alpha_2 - \alpha_3 = 3\alpha_2 - \alpha_3 = \alpha_2 - 2s\alpha_1 - \alpha_3 = -r\alpha_1 - \alpha_6 \\
 = -r\alpha_1 - \alpha_7,
 \end{aligned}$$

$$\alpha_1 + \alpha_2 - \alpha_3 - \alpha_6 = 2\alpha_2 - \alpha_6 = -\alpha_6 = 4\alpha_2 - 2\alpha_3 = 2\alpha_2 - \alpha_7,$$

$$\alpha_1 + \alpha_2 - \alpha_3 - \alpha_7 = 2\alpha_2 - \alpha_7 = -\alpha_7 = 2\alpha_2 - \alpha_6,$$

$$\alpha_2 - \alpha_3 = -m\alpha_1, \quad \alpha_1 - \alpha_3 = -n\alpha_1.$$

This relation gives

$$\begin{aligned}
 \alpha_2 = \frac{(1-m)}{2} \alpha_1, \quad \alpha_3 = \frac{(1+m)}{2} \alpha_1, \quad \alpha_4 = m \alpha_1, \quad \alpha_5 = \frac{(m-1)}{2} \alpha_1, \quad \alpha_6 = 0, \\
 \alpha_7 = 0, \quad s = \frac{m-1}{2}, \quad n = \frac{m-1}{2}, \quad r = 2m - 1.
 \end{aligned} \tag{16}$$

It can be seen from equation (16) that when the sheet is stretched with a speed $U(x) = C_1 x^m$, there exists a similarity solution to this problem provided that:

$$B(x) = B_0 x^{\frac{(m-1)}{2}}, \quad v_w = C_2 x^{\frac{(m-1)}{2}} . \tag{17}$$

Thus the set Γ reduces to a one parameter group transformation as

$$\begin{aligned}
 \Gamma: \quad x^* = x e^{\varepsilon\alpha_1}, \quad y^* = y e^{\varepsilon \frac{(1-m)}{2} \alpha_1}, \quad \psi^* = \psi e^{\varepsilon \frac{(1+m)}{2} \alpha_1}, \\
 u^* = u e^{\varepsilon m \alpha_1}, \quad v^* = v e^{\varepsilon \frac{(m-1)}{2} \alpha_1}, \quad \theta^* = \theta, \quad \varphi^* = \varphi .
 \end{aligned} \tag{18}$$

Expanding by Taylor's method in powers of ε and keeping terms up to the order ε , we obtain

$$x^* - x = x\varepsilon\alpha_1, \quad y^* - y = y\varepsilon\frac{(1-m)}{2}\alpha_1, \quad \psi^* - \psi = \psi\varepsilon\frac{(1+m)}{2}\alpha_1,$$

$$u^* - u = u\varepsilon m\alpha_1, \quad v^* - v = v\varepsilon\frac{(m-1)}{2}\alpha_1, \quad \theta^* - \theta = 0, \quad \varphi^* - \varphi = 0.$$

After differentials, we yield

$$\frac{dx}{\alpha_1 x} = \frac{dy}{y\frac{(1-m)}{2}\alpha_1} = \frac{d\psi}{\psi\frac{(1+m)}{2}\alpha_1} = \frac{d\theta}{0} = \frac{d\varphi}{0}. \quad (19)$$

Solving the above equation, we obtain

$$\eta = yx^{\frac{m-1}{2}}, \quad \psi = x^{\frac{m+1}{2}}F(\eta), \quad \theta = \theta(\eta), \quad \varphi = \varphi(\eta). \quad (20)$$

Using these transformation equations (12) - (14) become

$$mF'^2 - \frac{(m+1)}{2}FF'' = vF''' - \frac{\sigma B_0^2}{\rho}F' + \frac{gB_T(T_w - T_\infty)}{x^{2m-1}}\theta + \frac{gB_C(C_w - C_\infty)}{x^{2m-1}}\varphi, \quad (21)$$

$$(2m-1)F'\theta - \frac{(m+1)}{2}F\theta' = \alpha\theta'' + \frac{D_m k_T(C_w - C_\infty)}{C_s C_p(T_w - T_\infty)}\varphi'' + \frac{Q_0 C_1 x}{\rho c_p U}\theta$$

$$+ \frac{vU^2}{c_p C_1^2(T_w - T_\infty)}F''^2, \quad (22)$$

$$(2m-1)F'\varphi - \frac{(m+1)}{2}F\varphi' = D_m\varphi'' + \frac{D_m k_T(T_w - T_\infty)}{T_m(C_w - C_\infty)}\theta'' - \frac{k^* C_1 x}{U}\varphi. \quad (23)$$

The boundary conditions are transformed to

$$\begin{aligned} F' = C_1, \quad F = f_w, \quad \theta = 1, \quad \varphi = 1 & \quad \text{at } \eta = 0, \\ F' \rightarrow 0, \quad \theta \rightarrow 0, \quad \varphi \rightarrow 0 & \quad \text{as } \eta \rightarrow \infty. \end{aligned} \quad (24)$$

Introducing the following transformations for η, F, θ and φ in equations (21)-(23)

$$\eta = v^\alpha C_1^\beta \eta^*, \quad F = v^{\alpha'} C_1^{\beta'} F^*, \quad \theta = v^{\alpha''} C_1^{\beta''} \theta^*, \quad \varphi = v^{\alpha'''} C_1^{\beta'''} \varphi^*,$$

we have

$$\alpha' = \alpha = 1/2, \quad \alpha'' = 0 = \alpha''', \quad \beta' = -\beta = 1/2, \quad \beta'' = 0 = \beta'''.$$

The equations (21)-(23) are transformed in to

$$mF^{*2} - \frac{(m+1)}{2}F^*F^{*''} = F^{*'''} - MF^{*'} + Gr\theta^* + Gc\varphi^*, \quad (25)$$

$$(2m-1)F^{*'}\theta^* - \frac{(m+1)}{2}F^*\theta^{*'} = \frac{1}{Pr}\theta^{*''} + Df\varphi^{*''} + \lambda\theta^* + EcF^{*''2}, \quad (26)$$

$$(2m-1)F^{*'}\varphi^* - \frac{(m+1)}{2}F^*\varphi^{*'} = \frac{1}{Sc}\varphi^{*''} + Sr\theta^{*''} - k\varphi^*, \quad (27)$$

where $M = \frac{\sigma B_0^2}{\rho C_1}$ is the magnetic parameter, $Gc = \frac{g^{BT}(T_w - T_\infty)}{C_1^2 x^{2m-1}}$ is the local modified Grashof number, $Gr = \frac{g^B C(C_w - C_\infty)}{C_1^2 x^{2m-1}}$ is the local Grashof number, $Pr = \frac{\nu}{\alpha}$ is the Prandtl number,

$$Df = \frac{D_m k_T (C_w - C_\infty)}{C_s C_p (T_w - T_\infty) \nu}$$

is the Dufour number, $Sr = \frac{D_m k_T (T_w - T_\infty)}{T_m (C_w - C_\infty) \nu}$ is the Soret number,

$$f_w = \left(-\frac{2C_2}{m+1} (\nu C_1)^{\frac{-1}{2}}\right)$$

is the suction or injection parameter, $Sc = \frac{\nu}{D_m}$ is the Schmidt number, $Ec = \frac{U^2}{c_p(T_w - T_\infty)}$ is the Eckert number, $\lambda = \frac{Q_0 x}{\rho c_p U}$ is heat source/sink parameter and $k = \frac{k^* x}{U}$ is chemical reaction parameter.

Let $F^* = f$, $\theta^* = \theta$ and $\varphi^* = \varphi$. Then equations (25)-(27) finally become

$$f''' + \frac{(m+1)}{2} f f'' - m f'^2 - M f' + Gr \theta + Gc \varphi = 0, \tag{28}$$

$$\frac{1}{Pr} \theta'' - (2m - 1) f' \theta + \frac{(m+1)}{2} f \theta' + Df \varphi'' + \lambda \theta + Ec f''^2 = 0, \tag{29}$$

$$\frac{1}{Sc} \varphi'' - (2m - 1) f' \varphi + \frac{(m+1)}{2} f \varphi' + Sr \theta'' - k \varphi = 0. \tag{30}$$

The corresponding boundary conditions take the form

$$\begin{aligned} f' = 1, \quad f = f_w, \quad \theta = 1, \quad \varphi = 1, \quad \text{at } \eta = 0, \\ f' = 0, \quad \theta = 0, \quad \varphi = 0, \quad \text{at } \eta \rightarrow \infty. \end{aligned} \tag{31}$$

The quantities of physical interest in this problem are the local skin friction coefficient, the local Nusselt number and the local Sherwood numbers, which are defined by

$$\begin{aligned} C_f = \frac{\tau_w}{\left(\frac{\rho U^2}{2}\right)} = 2Re_x^{-\frac{1}{2}} f''(0), \quad Nu = \frac{x q_w}{k(T_w - T_\infty)} = -Re_x^{-\frac{1}{2}} \theta'(0) \quad \text{and} \\ Sh = \frac{x m_w}{D_m (C_w - C_\infty)} = -Re_x^{-\frac{1}{2}} \varphi'(0), \end{aligned}$$

where

$$\tau_w = \mu \left(\frac{\partial u}{\partial y}\right)(x, 0), \quad q_w = -k \left(\frac{\partial T}{\partial y}\right)(x, 0) \quad \text{and} \quad m_w = -D_m \left(\frac{\partial C}{\partial y}\right)(x, 0).$$

3. Numerical method for solution

The non-linear boundary value problem represented by equations (28)-(30) is solved numerically using the Keller box method. The method has the following four main steps:

- i.. Reduce the equation or system of equations to a first order system;
- ii. Write the difference equations using central differences;
- iii. Linearize the resulting algebraic equations (if they are non-linear) by Newton's method write them in matrix-vector form;
- iv. Use the block-tridiagonal-elimination technique to solve the linear system.

In solving the system of non-linear ordinary differential equations (28)-(30) together with the boundary condition (31) using the Keller box method, the choice of an initial guess is very important in this scheme. The success of this method depends greatly on how much good this guess is to give the most accurate solution. Thus we made an initial guess of

$$f_0(\eta) = 1 + f_w - e^{-\eta}, \quad \theta_0(\eta) = e^{-\eta}, \quad \varphi_0(\eta) = e^{-\eta}. \quad (32)$$

This choice has been made on the convergence criteria together with the boundary conditions in consideration. As in Cebeci and Pradshaw (1988), the values of the wall shear stress, in our case $f''(0)$ is commonly used as a convergence criteria. This is because in the boundary layer calculations the greatest error appears in the wall shear stress parameter. In the present study this convergence criteria is used. In this study a uniform, grid size $\Delta\eta = 0.01$ is chosen to satisfy the convergence criteria of 10^{-4} , which gives about a four decimal places accuracy for most of the prescribed quantities.

4. Results and Discussion

In order to analyze the results, the numerical computations have been carried out using the method described in the previous section for various values of the flow parameters. For illustration of the results, numerical values are plotted in figures 1-9. The physical explanations of the appropriate change of parameters are given below. The values of local-skin friction coefficient $f''(0)$, temperature gradient $-\theta'(0)$ and mass transfer rate $-\varphi'(0)$ are tabulated in Table 1. From the Table, it is noticed the local the skin-friction coefficient $f''(0)$ increases with the increase of the flow parameters f_w, Gr, Gc, Sr, Df, Ec and decreases with the increase of Pr, Sc, m, M, k_1 . From the same table, it is observed that Nusselt number coefficient $-\theta'(0)$ increases with the increase of Pr, m, Gr, Gc, Sr , and suction parameter ($f_w > 0$) whereas it decreases with the increase of $Sc, M, Df, Ec, k_1, \lambda$ and injection parameter ($f_w < 0$). Lastly, it is also notice that the Sherwood number coefficient $-\varphi'(0)$ increases with the increase of $Sc, m, Gr, Gc, Df, Ec, k_1, \lambda$ and suction/injection parameter f_w and it decreases with the increase of Pr, M and Sr .

Table 1. The values of Skin-friction coefficient $f''(0)$, Nusselt number coefficient $-\theta'(0)$ and Sherwood number coefficient $-\phi'(0)$ for different values of the flow parameters.

Pr	Sc	m	Gr	Gc	M	f_w	Sr	Df	λ	Ec	k_1	$f''(0)$	$-\theta'(0)$	$-\phi'(0)$
0.71	0.22	1	2	10	0.5	0.5	0.4	0.15	0.2	0.03	0.3	3.7417	1.3656	0.7172
3	0.22	1	2	10	0.5	0.5	0.4	0.15	0.2	0.03	0.3	3.6005	3.2015	0.5596
7	0.22	1	2	10	0.5	0.5	0.4	0.15	0.2	0.03	0.3	3.5332	5.7752	0.3355
0.71	0.98	1	2	10	0.5	0.5	0.4	0.15	0.2	0.03	0.3	2.6231	1.1620	1.5229
0.71	0.22	2	2	10	0.5	0.5	0.4	0.15	0.2	0.03	0.3	2.3772	2.0139	0.9675
0.71	0.22	1	3	10	0.5	0.5	0.4	0.15	0.2	0.03	0.3	4.0206	1.3733	0.7231
0.71	0.22	1	2	7	0.5	0.5	0.4	0.15	0.2	0.03	0.3	2.6077	1.3107	0.6773
0.71	0.22	1	2	10	3	0.5	0.4	0.15	0.2	0.03	0.3	2.1978	1.2647	0.6463
0.71	0.22	1	2	10	0	0.5	0.4	0.15	0.2	0.03	0.3	4.1276	1.3857	0.7345
0.71	0.22	1	2	10	0.5	0.3	0.4	0.15	0.2	0.03	0.3	3.7020	1.2863	0.7043
0.71	0.22	1	2	10	0.5	0.5	2	0.15	0.2	0.03	0.3	4.1586	1.4212	0.4051
0.71	0.22	1	2	10	0.5	-0.3	0.4	0.15	0.2	0.03	0.3	3.4607	1.3866	0.6072
0.71	0.22	1	2	10	0.5	-0.5	0.4	0.15	0.2	0.03	0.3	3.3731	1.4408	0.5738
0.71	0.22	1	2	10	0.5	0.5	0.4	1	0.2	0.03	0.3	3.7800	1.1653	0.7352
0.71	0.22	1	2	10	0.5	0.5	0.4	0.15	0.4	0.03	0.3	3.7479	1.3090	0.7221
0.71	0.22	1	2	10	0.5	0.5	0.4	0.15	0.2	0.5	0.3	3.7922	0.7172	0.7740
0.71	0.22	1	2	10	0.5	0.5	0.4	0.15	0.2	0.03	0.5	3.6951	1.3586	0.7456

Figures 1a–1c show typical steady-state fluid tangential velocity, temperature and concentration for various values of the magnetic parameter M respectively. Application of a transverse magnetic field normal to the flow direction gives rise to a resistive drag-like force acting in a direction opposite to that of the flow. This has a tendency to reduce the fluid tangential velocity at the expense of increasing its temperature and the solute concentration. Also, the effects on the flow and thermal fields become more so as the strength of the magnetic field increases. Figures 2a-2c depicts the velocity, the temperature and the concentration profiles for different values of index parameter m respectively. It is observed that the velocity, the temperature and the concentration boundary layer decrease by increasing of the index parameter.

The effects of chemical reaction parameter k_1 on the velocity, temperature as well as concentration distributions are displayed in Figures 3a-3c, respectively. It should be noted that physically, positive values of k_1 implies destructive reaction and negative values of k_1 implies generative reaction. It is observed from these figures that an increase in the chemical reaction parameter k_1 leads to the decrease of the velocity and concentration profiles but it leads to increase in the temperature profiles. This shows that diffusion rate can be tremendously altered by chemical reaction. The effect of increasing the value of the heat generation/absorption parameter λ on the velocity is shown in Figure 4a. It is evident from this that increasing the value of the absorption of the radiation parameter due to increase in the buoyancy force accelerates the flow rate. The effect of absorption of radiation parameter on the temperature profiles is shown on Figure 4b.

It is seen from this figure that the effect of absorption of radiation is to increase temperature in the boundary layer as the radiated heat is absorbed by the fluid which in turn increases the temperature of the fluid very close to the boundary layer and its effect diminishes far away from the boundary

layer. Figures 5a -5c depict the velocity, the temperature and the concentration profiles for different values of suction/injection parameter. It is observed that the velocity, temperature and concentration profiles decrease by increasing of suction parameter/injection parameter. The influence of Soret number Sr and Dufour number Df on the dimensionless velocity, temperature and concentration are shown in Figures 6a, 6b and 6c respectively. The Soret number Sr defines the effect of the temperature gradients inducing significant mass diffusion effects. It is noticed that an increase in the Soret number Sr results an increase in the velocity and concentration within the boundary layer whereas it results in decreasing of the temperature profiles. The Dufour number Df signifies the contribution of the concentration gradients to the thermal energy flux in the flow. It is observed that an increase in the Dufour number causes a rise in the velocity and temperature throughout the boundary layer whereas it causes to decrease the concentration profiles. The influence of the Schmidt number Sc on the velocity, temperature and concentration profiles are plotted in Figures 7a, 7b and 7c respectively. The Schmidt number embodies the ratio of the momentum to the mass diffusivity. The Schmidt number therefore quantifies the relative effectiveness of momentum and mass transport by diffusion in the hydrodynamic (velocity) and concentration (species) boundary layers. As the Schmidt number increases the concentration decreases. This causes the concentration buoyancy effects to decrease yielding a reduce in the fluid velocity.

The reductions in the velocity and concentration profiles are accompanied by simultaneous reductions in the velocity and concentration boundary as it is observed in Figure 7b. For different values of the Prandtl number Pr , the velocity and temperature profiles are plotted in Figure 8a and 8b respectively. The Prandtl number defines the ratio of momentum diffusivity to thermal diffusivity. From Figure 8a, it is clear that an increase in the Prandtl number leads to a fall in the velocity. From Figure 8b, it is observed that an increase in the Prandtl number results a decrease of the thermal boundary layer thickness. The reason is that smaller values of Pr are equivalent to increasing the thermal conductivities and therefore heat is able to diffuse away from the heated surface more rapidly than for higher values of Pr . Hence in the case of smaller Prandtl numbers as the boundary layer is thicker and the rate of heat transfer is reduced. The influence of Eckert number Ec on the dimensionless temperature function is shown in Figure 9. The Eckert number designates the ratio of the kinetic energy of the flow to the boundary layer enthalpy difference. It embodies the conversion of kinetic energy into internal energy by work done against the viscous fluid stresses. The positive Eckert number implies cooling of the plate i.e., loss of heat from the plate to the fluid. Hence, greater viscous dissipative heat causes a rise in the temperature as well as the velocity which is evident from Figure 9.

5. Conclusion

In this paper, scaling group analysis on MHD free convective heat and mass transfer over a stretching surface considering suction or injection, heat source/sink, viscous dissipation and chemical reaction is investigated. Efficient method of Lie group analysis is used to solve the governing equations of motion. This procedure helps in removing the difficulties faced in solving the equations arising from the non-linear character of the partial differential equations. The scaling symmetry group is very essential procedure to comprehend the mathematical model and to find the similarity solutions for such type of flow which have wider applications in the engineering disciplines related to fluid mechanics. This reduces the system of non-linear coupled partial differential equations governing the motion of the fluid in to a system of coupled

ordinary differential equations by reducing the number of independent variables. The transformed governing equations in the present study were solved numerically by using the Keller box method. From the present study the following conclusion can be drawn:

- i. The influence of magnetic field parameter is to reduce velocity profiles whereas temperature and concentration profiles increase.
- ii. A positive increase in Eckert number is shown to reduce the temperature profile in the flow.
- iii. Increasing the Prandtl number substantially decreases the velocity and the temperature in the flow.
- iv. An increase of Schmidt numbers causes a decline in the velocity as well as the concentration profiles whereas it causes to increase the temperature profiles
- v. An increase in Dufour number causes a rise in the velocity and temperature throughout the boundary layer whereas it causes to decrease the concentration profiles
- vi. An increase in the Soret number is to increase in the velocity and concentration within the boundary and is to decrease the temperature profiles.
- vii. An increase of chemical reaction parameter is to decrease the velocity and concentration profiles and is to increase the temperature profiles in the flow.
- viii. It is found that the velocity and temperature profiles in the flow increase with the increase of heat generation parameter.
- ix. It is observed that the velocity, temperature and concentration profiles decrease by increasing of suction parameter/injection parameter in the flow.

REFERENCES

- Alam, M.S., Rahman, M.M., Abddul M.M and Ferdows, M. (2006). Dufour and Soret effects on steady MHD combined free-forced convective and mass transfer flow past a semi-infinite vertical plate, *Thammasat Int J Sci* Vol. 11, pp.1-12.
- Alam, M.S., Rahman, M.M. and Abddul M.M. (2005). Local Similarity solutions for unsteady MHD free convection and mass transfer flow past an impulsively started vertical porous plate with Dufour and Soret effects, *Thammasat Int J Sci Tech*, Vol. 10, pp. 1-8
- Afify, A. A. (2004). MHD free convective flow and mass transfer over a stretching sheet with chemical reaction, *Heat and Mass Transfer*, Vol.40, No.6, pp. 495–500.
- Anghel, M., Takhar, H.S, and Pop, I. (2000). Dufour and Soret Effects on free convection boundary layer over a vertical surface embedded in a porous mediem, *J. Heat and Mass Transfer*, Vol.43, pp. 1265-1274.
- Ali, M. E. (1996).The effect of suction or injection on the Laminar boundary layer development over a stretched surface, *journal of Engineering Sciences King Saud University*,Vol.8, pp.43–58.
- Crane, L. J. (1970). Flow past a stretching plate, *Journal of Applied Mathematics and Physics* Vol.21, pp.645–647.

- Chiam, Tc. (1995). Hydrodynamic flow over a surface stretching with a power law velocity, *Int J Eng Sci*, Vol. 33, pp. 429-435.
- Chamkha, A. J. (2003). MHD flow of a uniformly stretched vertical permeable surface in the presence of heat generation/absorption and a chemical reaction, *International Communications in Heat and Mass Transfer*, Vol.30, No.3, pp. 413–422
- Cebeci, T. and Pradshaw, P. (1988). *Physical and computational Aspects of Convective Heat Transfer*, Springer, New York.
- Erickson, L. E., Fan, L. T. and Fox, V. G. (1966). Heat and mass transfer on a moving continuous flat plate with suction or injection, *Industrial and Engineering Chemistry Fundamentals*, Vol. 5, No.1, pp. 19–25.
- Dursunkaya, Z. and Worek, W.M. (1992). Diffusion –thermo and thermal diffusion effects in transient and steady natural convection from a vertical surface, *Int J. Heat Mass Transfer*, Vol.35, pp. 2060-2065. Dio: 10.1016/0017-9310(92)90208-A
- Fox, V. G., Erickson, L. E. and Fan, L. T. (1969). Methods for solving the boundary layer equations for moving continuous flat surfaces with suction and injection, *AIChE Journal*, Vol.14, pp. 726–736.
- Gupta, P. S. and Gupta, A. S. (1977). Heat and mass transfer on a stretching sheet with suction or blowing, *The Canadian Journal of Chemical Engineering*, Vol.55, pp. 744–746.
- Grubka, L. J. and Bobba, K. M. (1985). Heat transfer characteristics of a continuous stretching surface with variable temperature, *Journal of Heat Transfer*, Vol. 107, No.1, pp. 248–250.
- Gupta, A.S. (1962). Laminar free convection flow of an electrically conducting fluid from a vertical plate with uniform surface heat flux and variable wall temperature in the presence of a magnetic field, *Zeitschrift f` Ur Angewandte Mathematik und Physik*, Vol. 13, pp. 324–333.
- Gorla, R.S.R, Abboud, D.E and Sarmah, A. (1998). Magneto-hydrodynamic flow over a vertical stretching surface with suction and blowing, *Heat Mass transfer*, Vol. 34, pp. 121-125
- Gebharat, B. (1962). Effects of viscous dissipation in natural convection. *J. Fluid Mech*, Vol.14, pp. 225-232.
- Gebharat, B. and Mollendorf, J. (1969). Viscous dissipation in external natural convection flows, *J. Fluid. Mech*, Vol.38, pp. 97-107
- Hajmohamma, R., Hajmohammadi, S., Nourazar, S.S. and Campo, A. (2014). Analytical solution for two-phase flow between two rotating cylinders filled with power law liquid and a micro layer of gas, *Journal of Mechanical Science and Technology*, Vol. 28 ,No.5,pp. 1849-1854 DOI: 10.1007/s12206-013-0913-y
- Hajmohammed, M.Rand Nourazar, S.S (2014). On the insertion of a thin gas layer in micro cylindrical Couette flows involvin g power-law liquids, *International Journal of Heat & Mass Transfer*, Vol.75, pp. 97 -108
- Israel-Cookey, C., Ogulu, A.and Omubo-Pepple, V.B. (2003). Influence of viscous dissipation on unsteady MHD free-convection flow past an infinite heated vertical plate in porous medium with time-dependent suction, *Int. J. Heat Mass transfer*, Vol.46, pp.2305-2311.
- Kafoussias, N.G. and Williams, E.M. (1995). Thermal-diffusion and Diffusion-thermo effects on free convective and mass transfer boundary layer flow with temperature dependent viscosity, *Int.J.Eng.Science*, Vol. 33, pp.369-1376. Dio: 10.1016/0020-7225(94)00132
- Kandasamy, R. and Palanimani, P. G. (2007). Effects of chemical reactions, heat, and mass transfer on nonlinear magnetohydrodynamic boundary layer flow over a wedge with a

- porous medium in the presence of ohmic heating and viscous dissipation, *Journal of Porous Media*, Vol.10, No.5, pp. 489–501.
- Keller, H.B. (1971). *A new difference scheme for parabolic problems: Numerical solutions of partial differential equations. II* (Hybbard, B.ed.). 327350. New York: Academic Press.
- Khan, Z.H, Rahim Gul and Khan, W.A. (2008). Effect of variable thermal conductivity on heat transfer from a hollow sphere with heat generation using homotopy perturbation method, *ASME , Heat Transfer Summer Conference*, pp.301-309.
- Layek, Mukhopadhyay, G.C, S, and Aamad, S.k. (2006). Scaling group of transformation for boundary layer stagnation-point flow through a porous medium towards a heated stretching sheet, *Math.Modeling and analysis*, Vol.11, No.2, pp.187-197
- Makinde, O.D, Khan, W.A and Khan, Z.H. (2013). Buoyancy effects on MHD stagnation point flow and heat transfer of a nanofluid past a convectively heated stretching/shrinking sheet, *International Journal of Heat and Mass Transfer*, Vol. 62, pp.526-533. <http://dx.doi.org/10.1016/j.ijheatmasstransfer.2013.03.049>
- Manjulatha, V., Varma, S.V.k and Raju, V.C.C. (2014). Effects of Radiation Absorption and Mass Transfer on the Free Convective Flow Passed a Vertical Flat Plate through a Porous Medium in an Aligned Magnetic Field, *Applications and Applied mathematics: An international journal*, Vol.9, No.1, pp.75-93.
- Noreen, S.A, Nadeem, S, Rizwan, U.H and Khan, Z.H. (2013). Radiation effects on MHD stagnation point flow of nanofluid towards a stretching, *Radiation effects on MHD stagnation point flow of nanofluid towards a stretching surface with convective boundary condition*, *Chinese Journal of Aeronautics*, Vol.26, No.6, pp.1389-1397.
- Pal, D. and Mondal, H. (2011). Effects of Soret Dufour, chemical reaction and thermal radiation on MHD non-Darcy unsteady mixed convective heat and mass transfer over a stretching sheet, *Communications in Nonlinear Science and Numerical Simulation*, Vol.16, No.4, pp. 1942–1958
- Poselnico, A. (2004). Influence of a magnetic field on heat and mass transfer by natural convection from vertical surfaces in porous media considering Soret and Dufour effects. *Int. J. Heat Mass transfer*, Vol. 47, pp.1467- 1472. doi:10.1016/j.ijheatmasstransfer,2003.09.017.
- Postelnicu, A. (2007). Influence of chemical reaction on heat and mass transfer by natural convection from vertical surfaces in porous media considering Soret and Dufour effects, *Heat and Mass Transfer*, Vol. 43, No.6, pp. 595–602.
- Prakash, J., Vijaya Kumar, A.G, Madhavi, M and Varma, S.V.K.(2014). Effects of Chemical Reaction and Radiation Absorption on MHD Flow of Dusty Viscoelastic Fluid, *Applications and Applied mathematics: An international Journal*, Vol.9, No.1, pp.141-156.
- Sakiadis, B. C. (1961). Boundary-layer behavior on continuous solid surfaces: I. Boundary-layer equations for two-dimensional and axisymmetric flow, *AIChE Journal*, Vol. 7, pp.26–28.
- Soundalgekar, V. M. and Murty, T. V. R. (1980). Heat transfer in MHD flow with pressure gradient, suction and injection, *Journal of Engineering Mathematics*, Vol.14, No.2, pp.155–158.
- Seddeek, M.A. (2004). Thermal-diffusion and diffusion – thermo effects on mixed free forced convective flow and mass transfer over accelerating surface with a heat source in the presence of suction and blowing in the case of variable viscosity, *Acta Mechanica*, Vol.172, pp. 83-94.

- Soundalgekar, V.M. (1972). Viscous dissipation effects on unsteady free convective flow past an infinite, vertical porous plate with constant suction, *Int. J. Heat Mass Transfer*, Vol. 15, pp. 1253-1261
- Tsou, F. K., Sparrow, E. M. and Goldstein, R. J. (1967). Flow and heat transfer in the boundary layer on a continuous moving surface, *International Journal of Heat and Mass Transfer*, Vol. 10, No. 2, pp. 219–235.
- Ullah, H., Islam, S., Idrees, M (2013). Solution of Boundary Layer Problems with Heat Transfer by Optimal Homotopy Asymptotic Method. *Abstract and Applied Analysis Volume 2013* Article ID 324869, 10 pages.
- Ullah, H., Islam, S., Idrees, M., Fiza, M., and Zeman, A. (2014). Three dimensional flow past a stretching sheet by extended optimal homotopy asymptotic method, *Sci.Int (Lahore)*, Vol.26, No.2, pp.567-576.

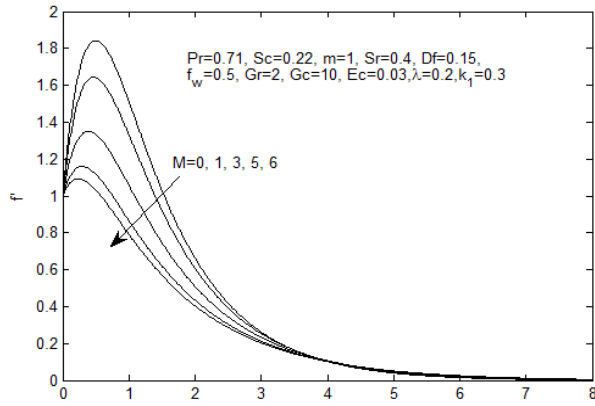


Figure.1a. Velocity profiles for different values of magnetic paramter M.

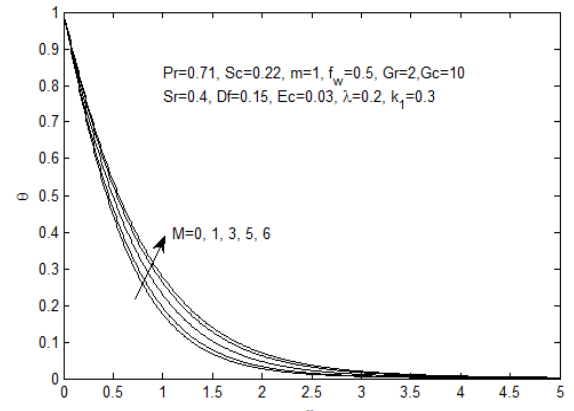


Figure.1b. Temperature profiles for different values of magnetic paramter M.

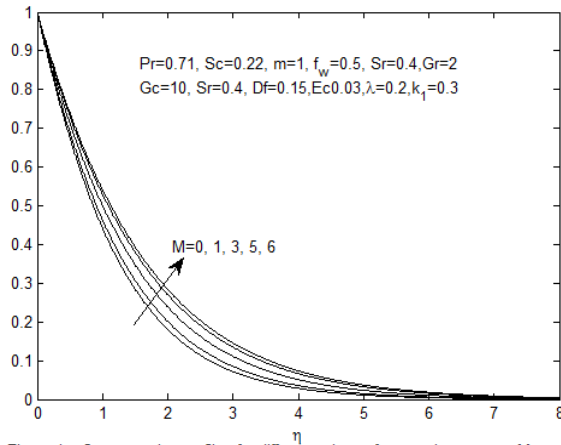


Figure.1c. Concentration profiles for different values of magnetic paramter M.

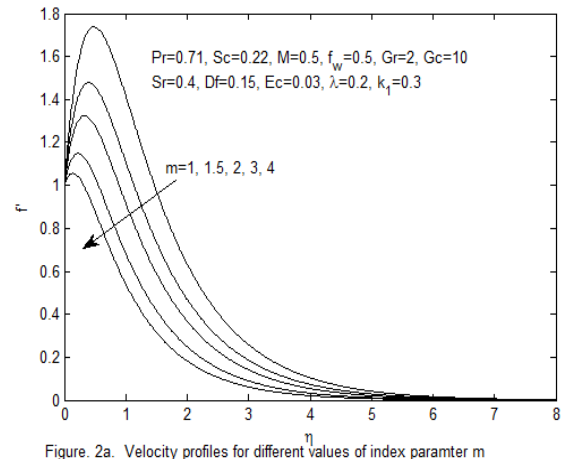


Figure. 2a. Velocity profiles for different values of index paramter m

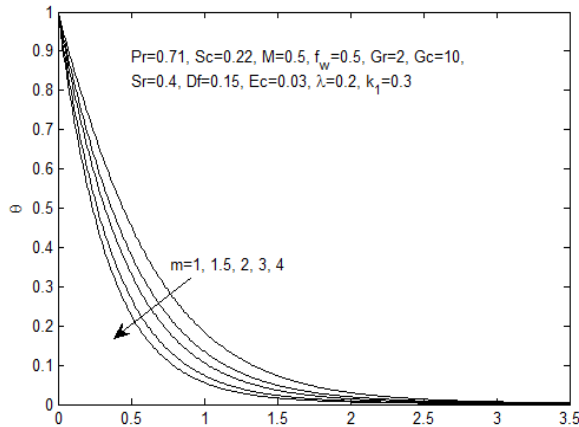


Figure.2b. Temperature profiles for different values of index paramter m

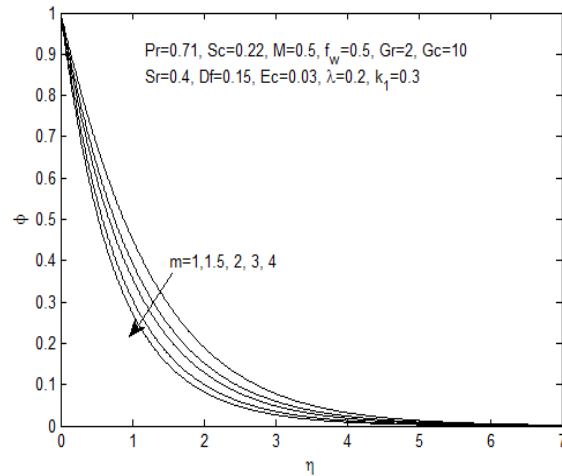


Figure. 2c. Concentration profiles for different values of index paramter

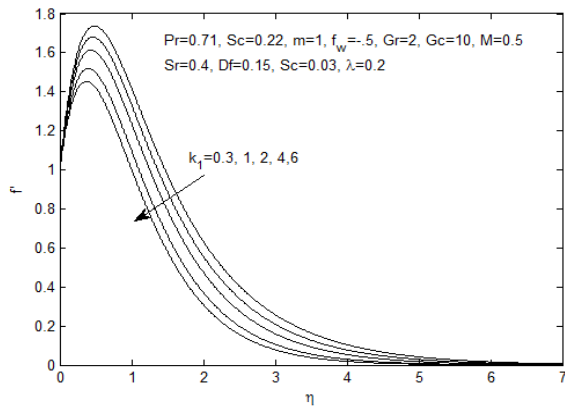


Figure.3a Velocity profiles for different values of chemical reaction parameter k_1

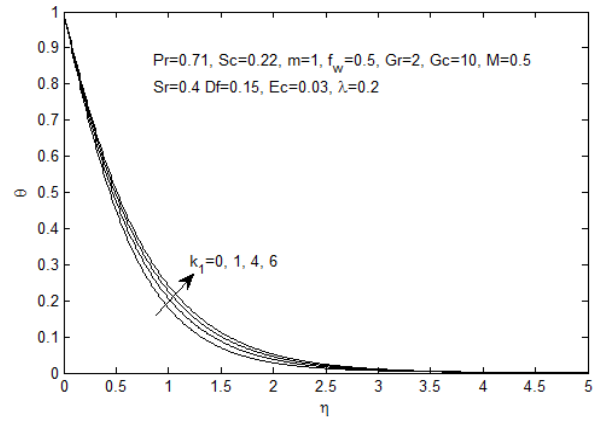


Figure.3b. Temperature profiles for different values of chemical reaction k_1

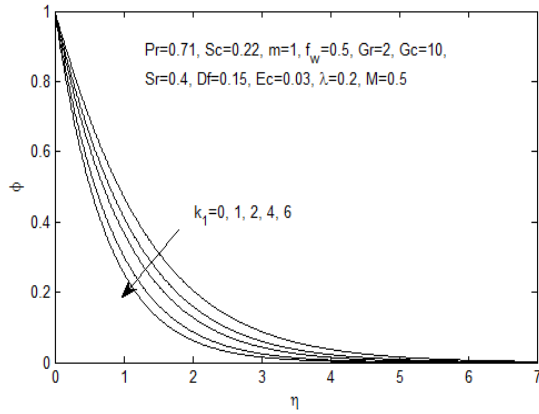


Figure.3c. Concentration profiles for different values of chemical reaction k_1

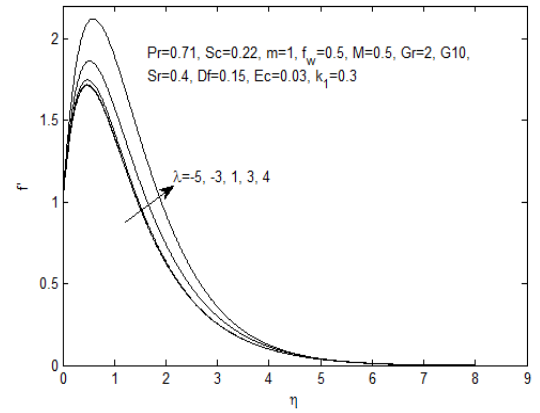


Figure.4a. Velocity profiles for different values of heat generation/absorption

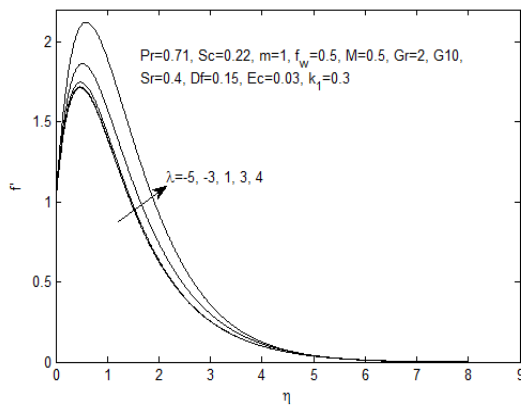


Figure.4a. Velocity profiles for different values of heat generation/absorption

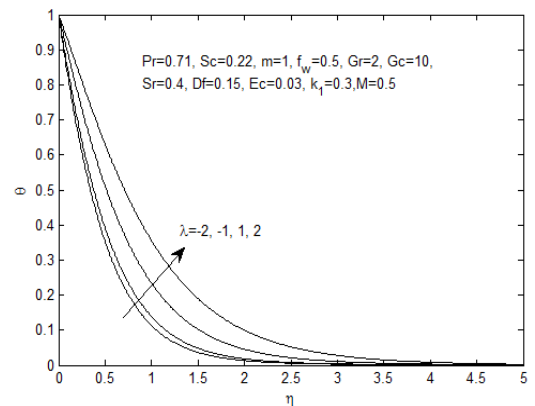


Figure.4b. Temperature profiles for different values of heat generation/absorption paramter

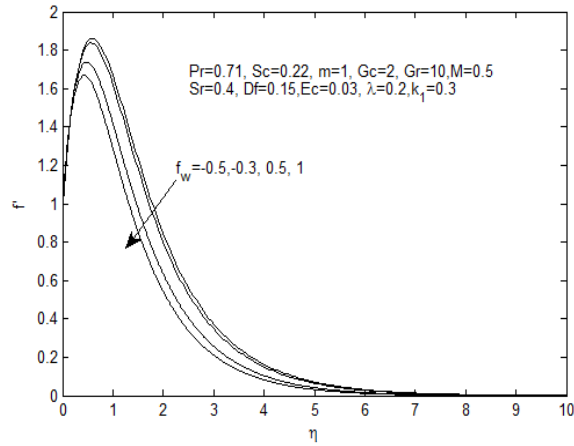


Figure 5a. Velocity profiles for different values of suction/injection parameter f_w

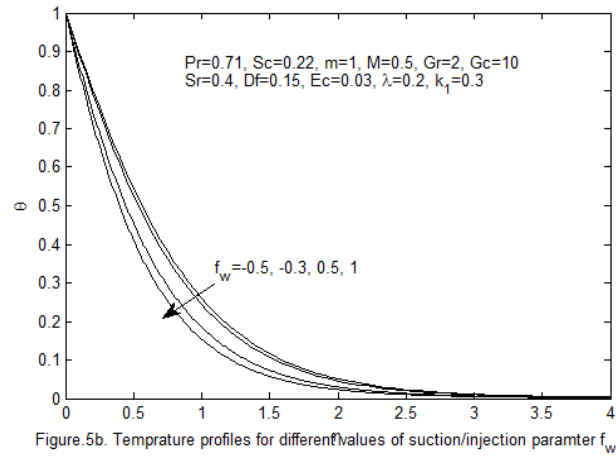


Figure 5b. Temperature profiles for different values of suction/injection parameter f_w

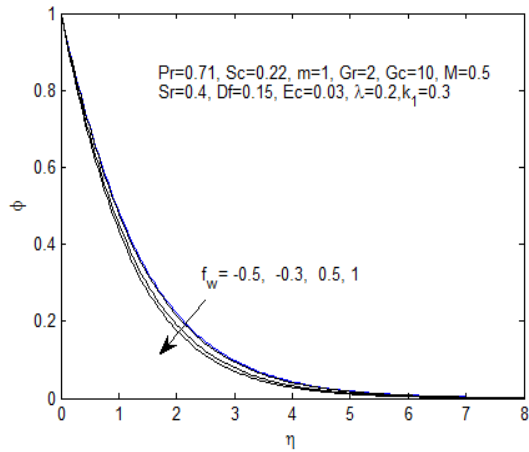


Figure 5c. Concentration profile for different values of suction/injection parameter f_w

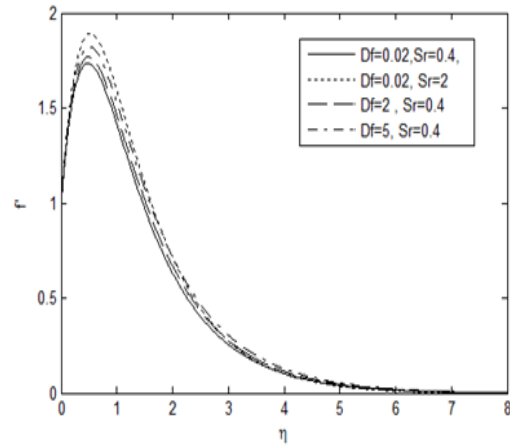


Figure 6a. Velocity profiles for different values of Df, Sr and for $Pr=0.71, Sc=0.22, Gr=2, Gc=10, m=1, M=0.5, Ec=0.03, \lambda=0.2, k_1=0.3$

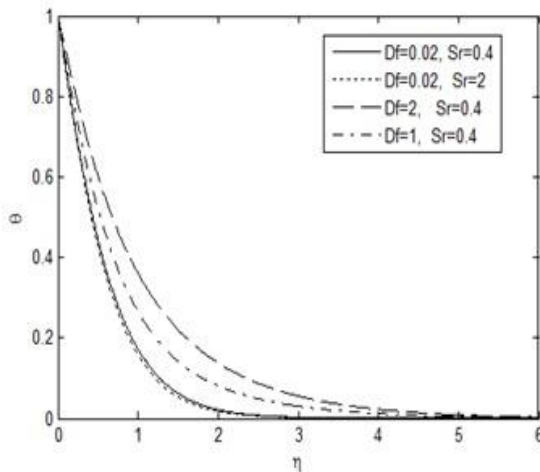


Figure 6b. Temperature profiles for different values of Df, Sr and for $Pr=0.71, Sc=0.22, m=1, M=0.5, Ec=0.03, k_1=0.3, \lambda=0.2, Gr=2, Gc=10$

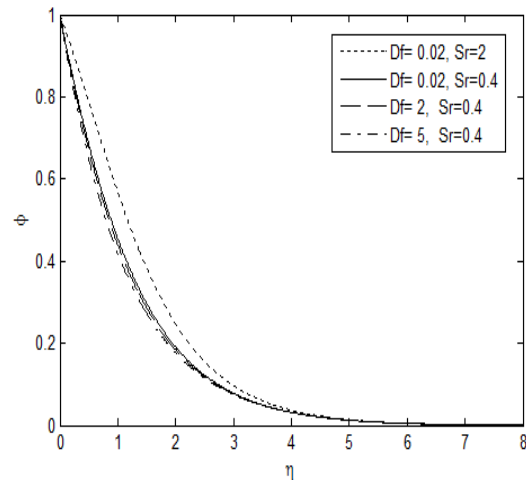


Figure 6c. Concentration profiles for different values of Df, Sr and for $Pr=0.71, Sc=0.22, m=1, M=0.5, Ec=0.03, k_1=0.3, \lambda=0.2, Gr=2, Gc=10$

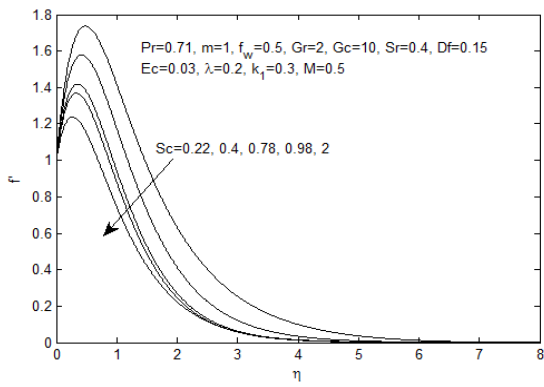


Figure. 7a. Velocity profiles for different values of Schmidt number

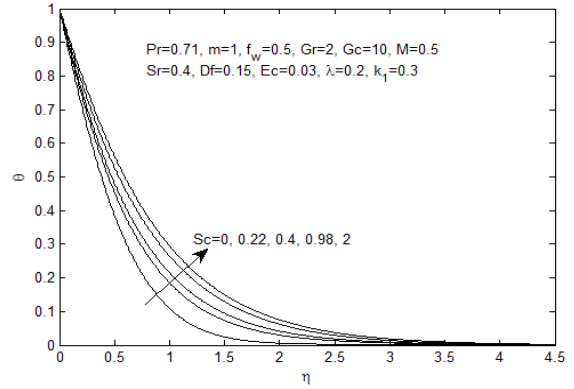


Figure. 7b. Temperature profiles for different values of Schmidt number

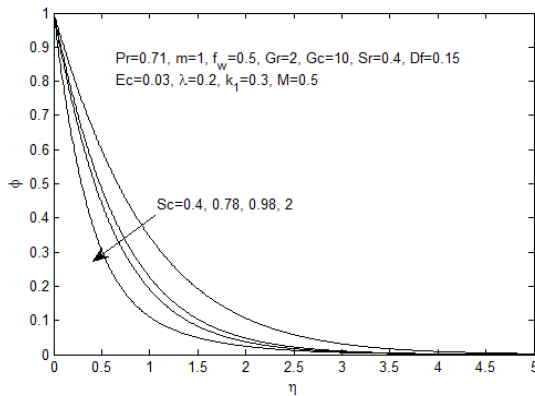


Figure. 7c. Concentration profiles for different values of Schmidt number

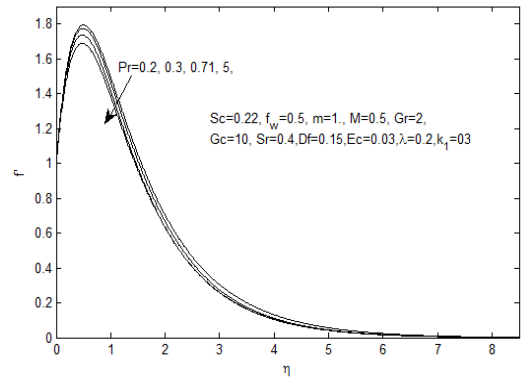


Figure. 8a. Velocity profiles for different values of Prandtl number Pr.

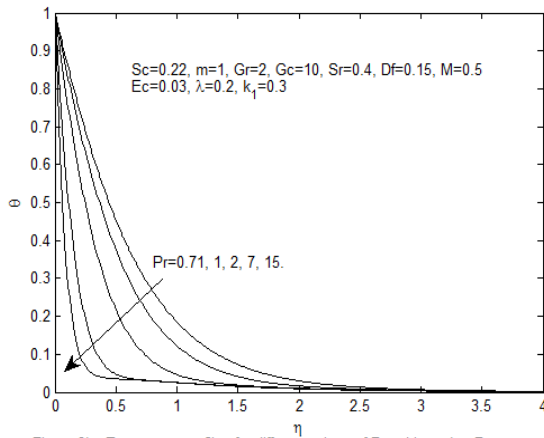


Figure. 8b. Temperature profiles for different values of Prandtl number Pr.

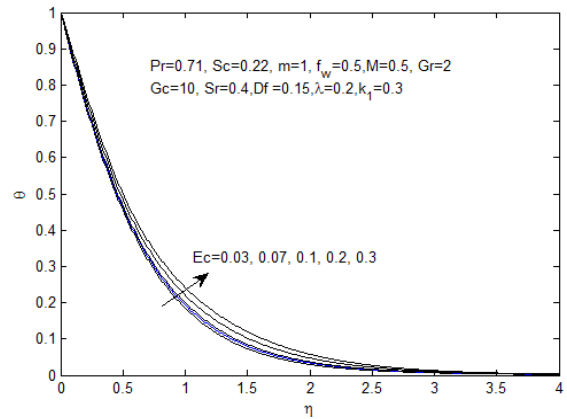


Figure. 9. Temperature profiles for different values of Eckert Number Ec.